Advances in Environmental Technology 12(1) 2026, 63-75.

Iranian Reasearch Organization for Science and Technology (IROST)

Advances in Environmental Technology

Journal home page: https://aet.irost.ir

Harnessing the impact of TiO_2 nanotubes, TiO_2 nanofibers and their incorporation in polysulfone composite membrane for the photocatalytic degradation of reactive black 5

Glanish Jude Martis[a], Arun M. Isloor[b]*, Sneha O[a], P. Satishkumar[b], Praveen S Mugali[a]

[a] *Department of P. G. Studies in Chemistry, Alva's College (Autonomous), Moodubidire, P. O. Box: 574 227, Dakshina Kannada, Karnataka, India.*

[b] *Membrane and Separation Technology Laboratory, Department of Chemistry, National Institute of Technology, Karnataka, P. O. Box: 575 025, Surathkal, Mangalore, India.*

ARTICLE INFO

Document Type:
Research Paper

Article history:
Received 06 April 2025
Received in revised form
15 December 2025
Accepted 20 December 2025

Keywords:
Nanotubes
Nanofibers
Polysulfone
Photocatalytic dye degradation
Reactive black 5

ABSTRACT

Most water resources today are contaminated for various reasons. Examples are dyes that pollute aquatic systems and threaten the environment. To overcome this problem, photocatalytic decomposition is a prominent method for eradicating hazardous dyes from water. The hydrothermal synthesis of TiO_2 nanotubes and nanofibers and their subsequent utility in degrading Reactive Black (RB) 5 dye is of great interest, and the resulting nanomaterials have been characterized and validated *via* various techniques: ultraviolet visible (UV-Vis) spectroscopy, X-ray diffraction (XRD), and scanning electron microscopy (SEM) with energy dispersive analysis (EDAX). Polysulfone (PSF) composite membranes lodged with synthesized nanomaterials were tested for the degradation of RB 5 dye. As a result, dye degradation of 89.8% and 80.2% was achieved with the TiO_2 nanofibers and TiO_2 nanotubes, respectively. When the nanomaterials were allowed to act upon the dye solution alone, the TiO_2 nanofibers degraded up to 48.7%, whereas the TiO_2 nanotubes degraded up to 18.6% because the strength of the nanomaterials was not enough for dye decomposition. This study reports on the synthesis and characterization of nanomaterials, as well as their combination for an enhanced dye degradation process.

1. Introduction

Synthetic dyes have various applications. At the same time, they pollute the environment by contaminating water bodies. The release of wastewater containing dyes from the textile industry has negative impacts and consequences on human health and the environment [1]. Due to improper monitoring of industrial release, estuaries in China and African countries have faced many hazardous effects [2]. Among the pollutants that

*Corresponding author Tel.: +91 9448523990
E-mail: isloor@yahoo.com
DOI: 10.22104/AET.2025.7536.2113

harm the environment, wastewater containing dyes is one of the prime polluters [3]. Hence, numerous experiments and studies have been conducted to remove or separate dyes from wastewater and treat them effectively [4–6]. In particular, organic and inorganic contaminants have been removed from water using biochar [7], cyclodextrin polyurethanes [8], seaweed biosorbents [9], among others. Another approach is the use of membrane technology for treating wastewater.

Membrane technology is one of the emerging technologies that is continually evolving, with its use in various applications to address the phenomenon of separation. However, the basic principle remains the same, even though the material characteristics apparently differ [10]. Membranes aid in the degradation of various dyes of commercial importance that are harmful when they are exposed to the human body. Polyaniline (PANI), polysulfone (PSF), and polyvinylpyrrolidone (PVP) membranes have been highly attractive because of their exciting polymeric structures [11]. PSF/TiO_2 hollow fiber membranes synthesized by Hamid *et al*. resulted in significant dye rejection in the removal of Humic acid [12].

The sharp characteristics and properties of PSF membranes, such as high chemical and thermal resistance with remarkable mechanical affinity, make them promising materials for research in membrane technology.

In addition, they are readily available, processed efficiently, and less expensive. However, various attempts have been made to develop methods to increase the hydrophilicity and porosity of the surface in the blending of polymers, their grafts, etc. [13]. Isloor *et al*. worked on various membrane-related topics, such as derivatives of chitosan[14,15], TiO_2 nanotubes [16], and polyamides [17] with PSF membranes, and the outcome significantly improved with increased performance.

Oily wastewater treatment is equally important as that of contaminant dye removal from the industrial release. Several studies have been conducted on the removal of oily contaminants using various photocatalysts, such as $BiVO_4$ [18], $BiVO_4$/rGO and $BiVO_4$/g-C_3N_4 [19], Bi_2WO_6 [20], and TiO_2/γ-Al_2O_3 [21,22], embedded with ceramic membranes.

Sneha *et al*. developed $CaCO_3$ and TiO_2 nanoparticles and embedded PSF membranes for the photocatalytic degradation of RB 5 dye where the direct incorporation of the nanoparticles yielded significant results [23]. In contrast, *Coprinus cinereus* peroxidase was used to optimize RB 5 [24].

The substantial improvement in membrane permeability with the use of nanocomposite membranes has successfully attracted much interest [25]. Seema *et al*. used humic acid-based biopolymeric membranes to effectively degrade methylene blue and rhodamine B [26]. Razmjou *et al*. incorporated TiO_2 nanoparticles into polyethersulfone composite membranes, studied their performance, and reported efficient thermal resistance [27]. Photocatalytic reactions have been used to remove bilge organic pollutants using TiO_2 [28]. Even the advanced photooxidation factors of photocatalytic reactions are useful in hybrid processes [29]. However, TiO_2 has been proven to be an excellent photocatalyst because of its ability to exhibit high photooxidation and recovery [30].

Polymeric membranes have been used for water purification and are highly necessary, as water sources are at risk of depletion in nature [31–33]. Among them, polysulfone-functionalized membranes are used in wastewater treatment protocols, due to their prominent chemical, mechanical, and thermal properties [34]. In this context, the goal of the study was to synthesize TiO_2 nanotubes, as well as nanofibers, and investigate the photocatalytic degradation of RB 5 with and without PSF membranes.

2. Materials and methods

2.1. TiO_2 nanotubes: Synthesis

Four grams of coexisted TiO_2 powders (mixture of Anatase and Rutile) were mixed with 60 ml of aq. NaOH (10 mol/dm^3) solution in a Teflon hydrothermal autoclave at 110 °C for 18 h. The alkali treatment on the powders was performed and rinsed with distilled water. The HCl solution (0.1 mol/dm^3) and distilled water were used for further rinsing until the pH level of 7 was attained. The

resulting white colored sample was dried at 70 °C for 6 h [35].

2.2. TiO_2 nanofibers: Synthesis

0.20 g of Anatase – TiO_2 powder was transferred into a Teflon hydrothermal autoclave, and it was filled with 1M aq. NaOH solution up to three-quarters of its holding capacity. It was then regulated in a muffle furnace at 150 °C for 20 h [36].

2.3. TiO_2 nanotubes and nanofibers for the photocatalytic degradation of RB 5 dye

The RB 5 dye solution was first prepared by taking 10 mg of the RB 5 dye in distilled water (1000 mL). TiO_2 nanotubes (150 mg) were added to the 10 ppm RB 5 (300 mL) dye solution. The structure of RB 5 is provided in Figure 1 [37].

Probe sonication of this solution was run for 20 minutes and transferred to the photocatalytic reactor for the photocatalytic reaction with the irradiation of UV light, and at regular intervals of 15 min.

Samples were collected until dye degradation was observed. The collected samples were centrifuged at 3000 rpm for 20 min. The supernatant samples were separated and subjected to UV-Visible spectroscopic analysis.

A similar process was undertaken using TiO_2 nanofibers. The extent of photodegradation was analyzed using UV-Visible spectroscopy. However, when conducting control studies in dark conditions, there was no observable degradation of the dye, and the results were similar to those of the RB 5 feed solution.

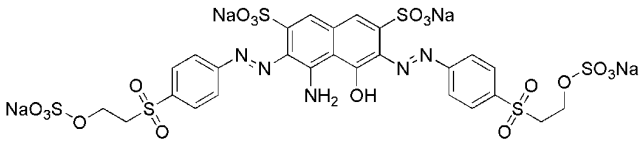

Fig. 1. Chemical Structure of Reactive Black 5

2.4. Preparation of TiO_2 nanotubes and nanofibers embedded PSF composite membranes

In-house synthesized 0.02 g of titanium dioxide nanotubes were added to a beaker containing 7.65 mL of N-Methylpyrrolidone (NMP) and sonicated for 30 min to achieve a homogenous distribution of the solution. Then, 2 g of PSF and 0.1 g of Polyvinylpyrrolidone (PVP) were added to the solution with constant stirring at 350 rpm at 55 °C for 24 h. The casting of the dope solution on the membrane caster was done carefully, and the resultant membrane was placed in the coagulation bath for 24 h [38].

A similar process was undertaken for the preparation of the TiO_2 nanofiber embedded PSF composite membrane. Using these fabricated membranes, the photocatalytic degradation of RB 5 dye was conducted.

2.5. Characterization of synthesized TiO_2 nanotubes and nanofibers

The synthesized TiO_2 nanotubes and nanofibers were characterized by XRD studies using Rigaku Miniflex (5^{th} generation).

The crystal structure of these nanomaterials was studied by the diffraction peaks obtained from this analysis. SEM analysis was carried out with ZEISS EVO MA18. The elemental composition of the surface of these nanomaterials was studied using an Oxford EDS (X-act) instrument.

The RB 5 dye was degraded photocatalytically using a photocatalytic reactor with a 125-250W UV-Visible tunable lamp. All the reactions were exposed to UV light for 90 minutes. The samples were collected every 30 minutes.

2.6. Contact angle measurement

To determine the membrane hydrophilicity, contact angle measurement was taken using a Kruss drop shape analyzer DS-100 instrument. Using the sessile droplet technique, 2.0 µL water droplet was placed on the dried TiO_2 nanotubes-PSF membrane.

The water contact angle was measured between the membrane surface under the water droplet and the tangent line at the edge of the water droplet where it touched the membrane surface.

3. Results and discussion

3.1. XRD analysis

The insights into the crystallographic structure of the synthesized TiO_2 nanotubes were obtained from the X-ray diffraction patterns. The diffracted peaks for both Rutile and Anatase forms are depicted in

Figure 2. The peaks at (011), (110), (004), (200), (020), (211), (024), and (221) crystal planes corresponded to the nanotubes. The 2θ peaks at 27.24°, 41.18°, 54.12°, and 68.82° confirmed the rutile structure, whereas those at 25.18°, 37.74°, 47.92°, and 62.58° confirmed the anatase structure. The crystallographic structure of the synthesized TiO_2 nanofibers from the XRD pattern is depicted in Figure 3. The peaks at (011), (044), (020), (121), (024), and (220) crystal planes correspond to the nanofibers. The anatase structure was confirmed by the obtained 2θ peaks at 25.02°, 37.52°, 47.74°, 54.78°, 62.52°, and 69.98.

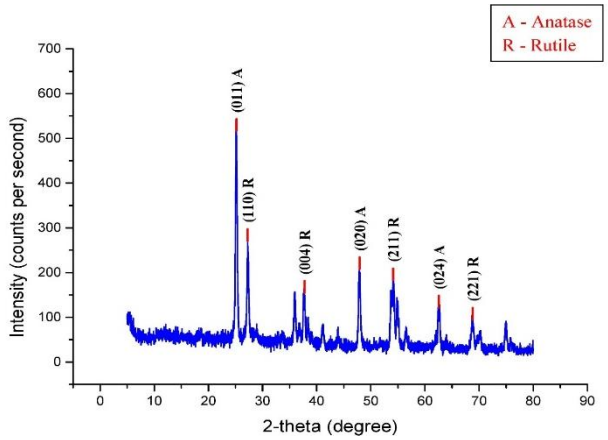

Fig. 2. X-ray diffraction pattern of TiO_2 nanotubes

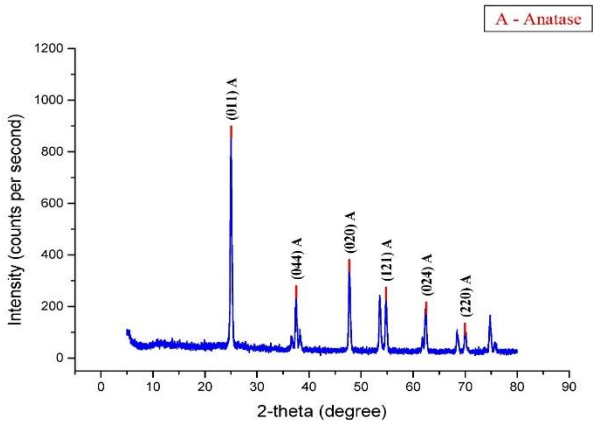

Fig. 3. X-ray diffraction pattern of TiO_2 nanofibers

3.2. SEM and EDAX analysis

The shape and morphology of the nanotubes and nanofibers were studied using the SEM micrographs captured at 35,000x magnification with a working distance of 7.5 mm.

From the SEM micrographs, it was evident that the nanotubes and nanofibers were in the nanometer range. The same has been presented in Figure 4.

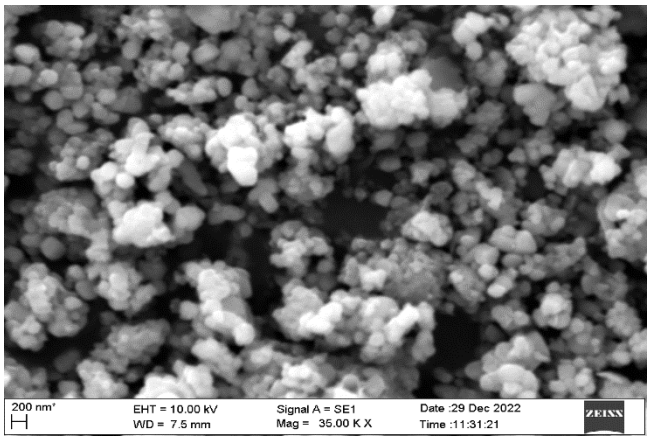

Fig. 4. a. SEM micrograph of TiO_2 nanotubes (area 1)

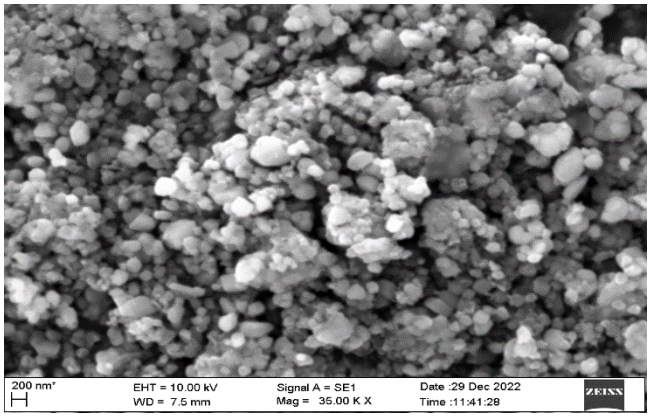

Fig.4. b. SEM micrograph of TiO_2 nanotubes (area 2)

The synthesized nanotubes were subjected to EDAX analysis for the elemental composition. The EDAX spectrum showed the presence of Ti and O, as illustrated in Figure 5. The peaks at 0.45 KeV and 4.56 KeV corresponded to the titanium of the K_α and L_α lines, respectively. The peak at 0.6 KeV was for oxygen. Other than these, there were no other peaks suggesting that the synthesized nanotubes were devoid of impurities. The weight percent of these nanotubes was determined to be 64.38% for titanium and 35.52% for oxygen.

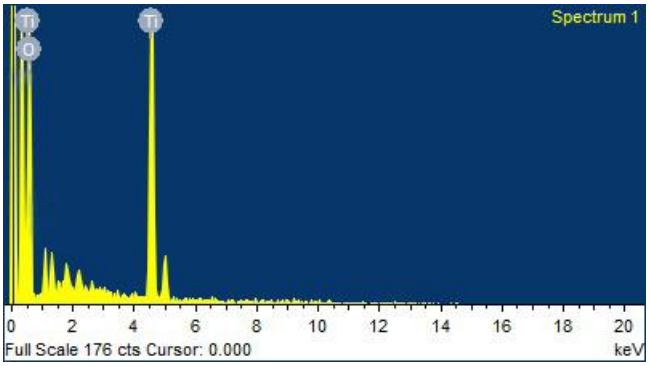

Fig. 5. EDAX spectrum of TiO_2 nanotubes

The SEM pictures of TiO_2 nanofibers are presented in Figure 6. Subsequently, the elemental composition of the synthesized nanofibers was analyzed. The EDAX spectrum showed the presence of Ti and O, as illustrated in Figure 7.

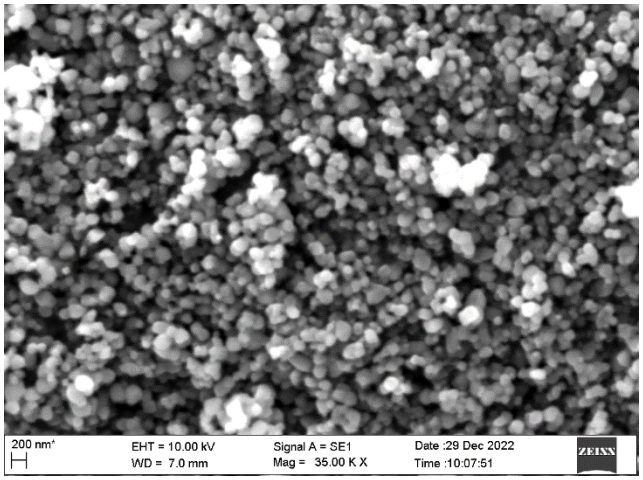

Fig. 6. a. SEM micrograph of TiO_2 Nanofibers (area 1)

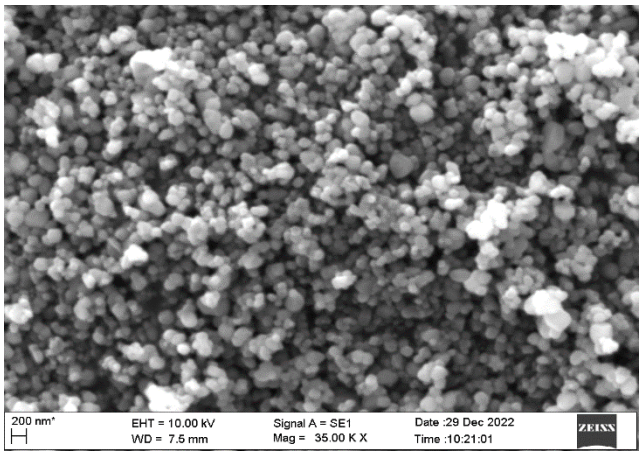

Fig. 6.b. SEM micrograph of TiO_2 Nanofibers (area 2)

The peaks at 0.40 KeV and 4.59 KeV corresponded to the titanium of the K_α and L_α lines, respectively. The peak at 0.57 KeV was for oxygen. Here too, the nanofibers were devoid of impurities, and the weight percent determination revealed 59.56% of titanium and 40.34% of oxygen.

TiO_2 nanotubes embedded with PSF membranes were examined with SEM analysis and the cross-sectional image of the membrane, as shown in Figure 8. Finger-like microvoids in the upper layer and the unsymmetrical structure with the macrovoids in the lower layer represent the typical morphology of the PSF membrane.

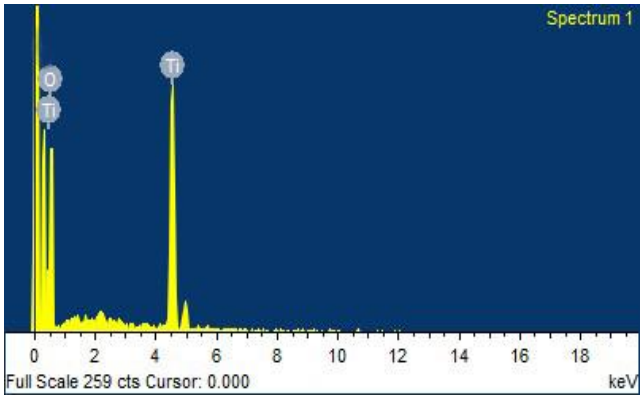

Fig. 7. EDAX spectrum of TiO_2 Nanofibers

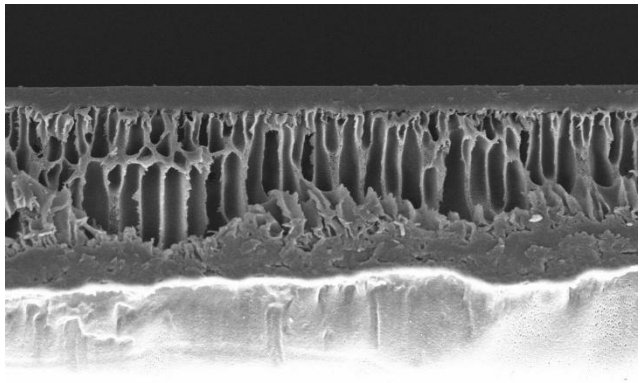

Fig. 8. Cross-sectional SEM micrograph of PSF membrane embedded with TiO_2 nanotubes

3.3. Contact angle measurement

A water contact angle of 74.8° was observed between the surface of the dried membrane under the water droplet and the tangent of the periphery of the water droplet where it meets the membrane surface, as depicted in Figure 9. This reveals the hydrophilic nature of the membrane surface, indicating higher resistance to the hydrophobic antifoulants.

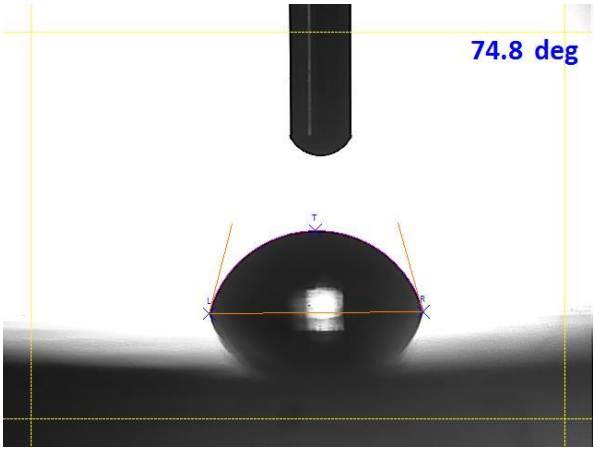

Fig. 9. Water contact angle measurement

3.4. Photocatalytic dye degradation

Photocatalysis is a process that uses light to initiate and accelerate the reaction. The mechanism behind the use of nanomaterials as effective photocatalysts is that when they are exposed to UV light, the absorption of photons leads to the excitation of electrons from the valence band to the conductance band. Additionally, this process leads to the formation of electron-hole pairs.

Reactive oxygen species (ROS) are essential for the photocatalytic decomposition of the dye. They are formed when excited electrons and hole pairs react with water and oxygen in the environment. These ROS could be hydroxyl radicals and superoxide anions. The plausible photocatalytic mechanism is illustrated in Figure 10, involving the photo-reduction of molecular oxygen to superoxide radical and its disproportionation to hydrogen peroxide. Likewise, photo-oxidation of the water molecule to hydrogen peroxide *via* dimerization of the hydroxyl radical is noteworthy.

UV-Visible spectroscopic analysis was performed on the feed solution of 10 ppm RB 5, and samples were collected at regular intervals of 30 mins. Figure 11 depicts the photocatalytic decomposition of RB 5 (10 ppm) with TiO_2 nanotubes without a membrane, represented as TNT WM at 30, 60, and 90 min.

This action was very low in decomposing the dye. The degradation was only 18.6%, as observed at 595 nm. Figure 12 shows the percentage degradation of RB 5 dye at intervals of 30, 60, and 90 min, respectively. Figure 13 illustrates the photocatalytic decomposition of 1.3 ppm RB 5 dye with TiO_2 nanotubes embedded with a PSF membrane at regular intervals of 30 mins.

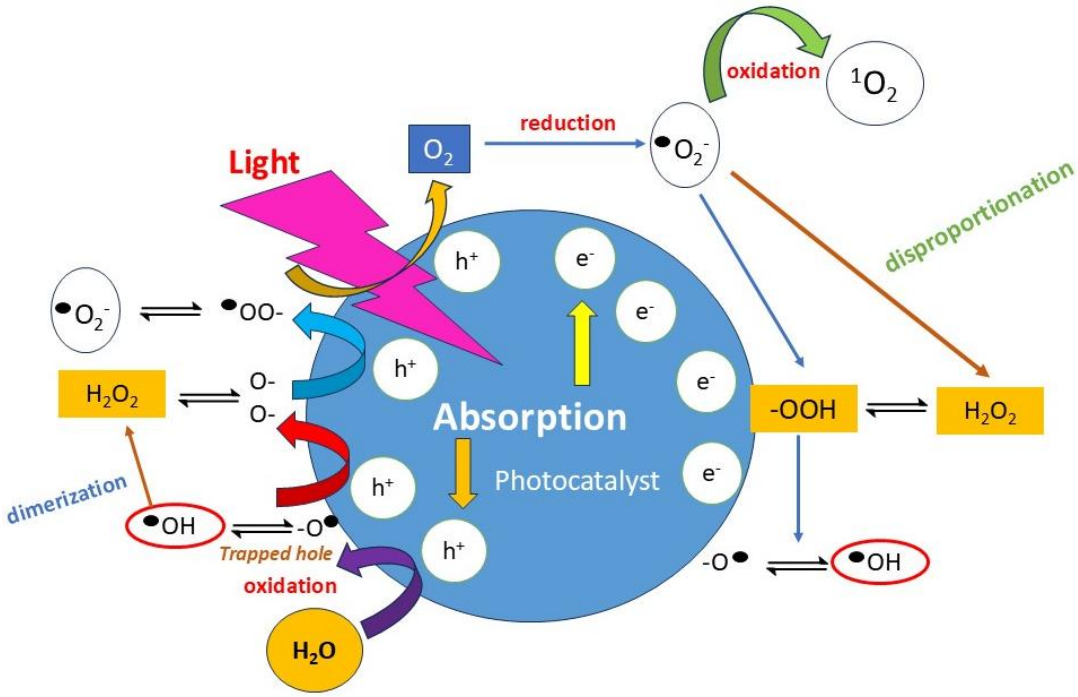

Fig. 10. Plausible mechanism of the photocatalytic reaction for the generation of ROS

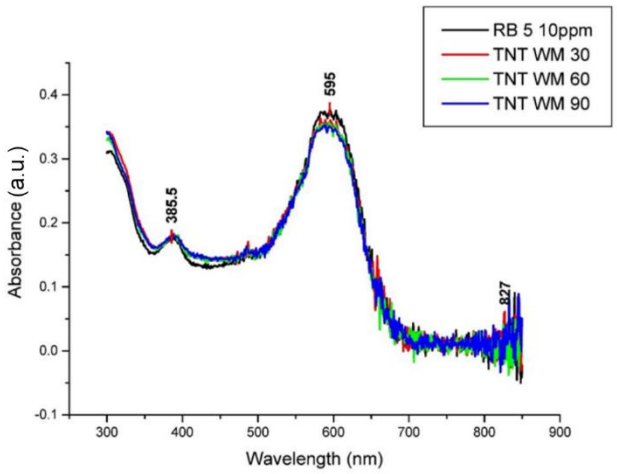

Fig. 11. Effect of TiO_2 nanotubes on RB 5 dye degradation

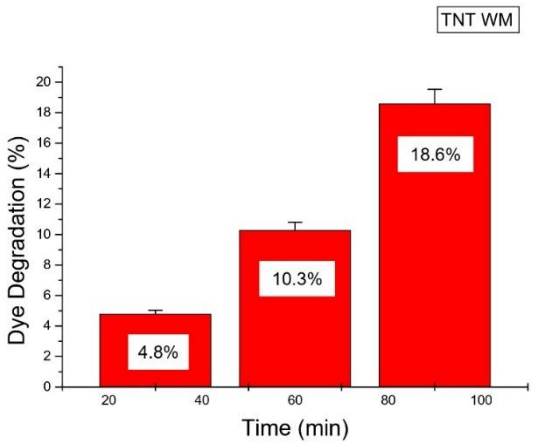

Fig. 12. Percentage degradation of RB 5 (10 ppm) with TiO_2 nanotubes. Error bars show standard deviations

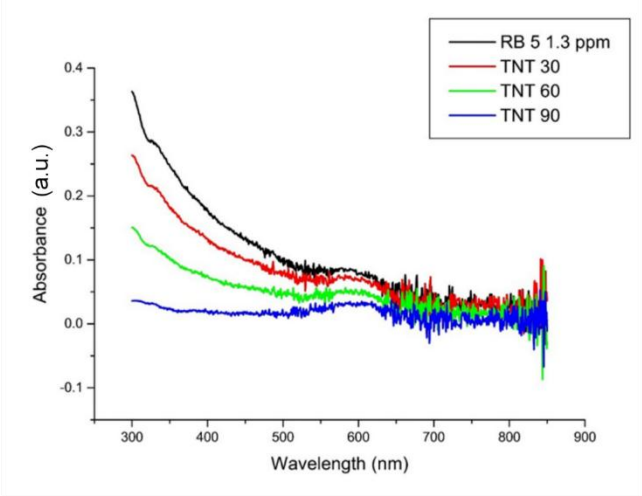

Fig. 13. Effect of TiO_2 nanotubes - PSF membrane on RB 5 dye degradation

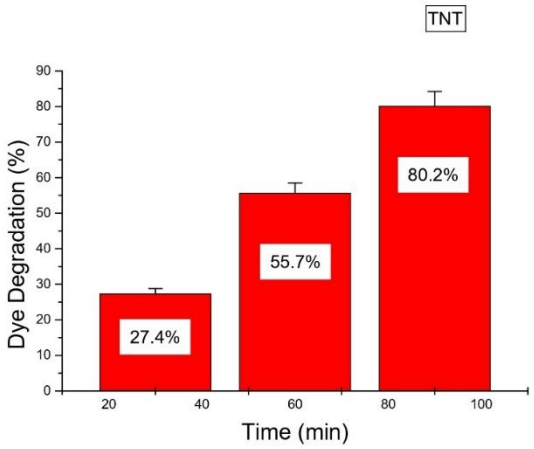

Fig. 14. Percentage degradation of RB 5 (1.3 ppm) with TiO_2 nanotubes – PSF membrane. Error bars show standard deviations

When PSF membranes are used, the number of nanomaterials available for catalysis is less. Moreover, the nanomaterials present at the extrinsic part play their role in catalysis. Therefore, the concentration of the dye solution is reduced to compare the performance of dye degradation.

Here, significant dye decomposition was found, i.e., 80.2%, when compared to that with TNT WM. The high degradation can be accounted for by the fact that the polymer matrix strengthened the nanotubes in degrading the dye. The polymeric membrane provided solid support by acting as a scaffold to the nano photocatalysts, enhancing the reaction rate and photocatalytic reaction.

The cleavage of the dye molecules by ROS on the surface of the composite membrane is another factor responsible for the enhanced dye degradation.

Apart from these, the surface morphology of the photocatalysts also contributes to the dye degradation embedded with the PSF membranes. Figure 14 shows the percentage degradation of RB 5 dye at intervals of 30, 60, and 90 min, respectively. Figure 15 emphasizes the photocatalytic decomposition of 10 ppm RB 5 with

TiO_2 nanofibers without membrane, represented as TNF WM at 30, 60, and 90 min. The effect was moderate, i.e., 48.7% of dye degradation was observed.

In comparison with the nanotubes, these nanofibers were quite efficient and a better photocatalyst. Figure 16 shows the percentage degradation of RB 5 dye at intervals of 30, 60, and 90 min, respectively.

Figure 17 shows the photocatalytic decomposition of 1.3 ppm RB 5 dye with TiO_2 Nanofibers embedded with a PSF membrane at regular intervals of 30 mins. Here, excellent dye decomposition was found, i.e., 89.8%, when compared to that with TNF WM. This promising degradation can be attributed to the fact that the polymer matrix strengthened the nanotubes in degrading the dye, as seen in the case of TNT WM. Figure 18 shows the percentage degradation of RB 5 dye at intervals of 30, 60, and 90 min, respectively.

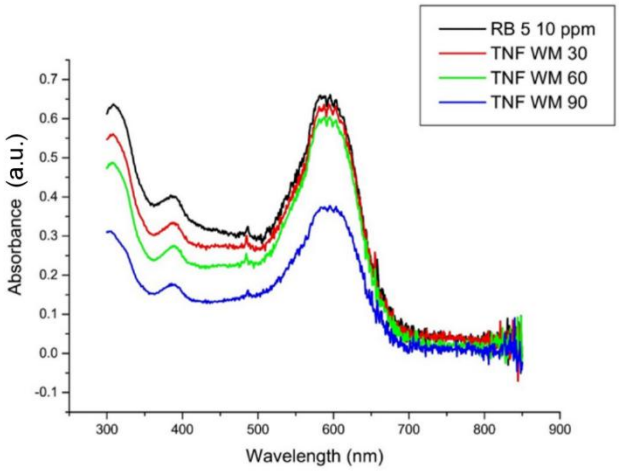

Fig. 15. Action of TiO_2 nanofibers on RB 5 dye degradation

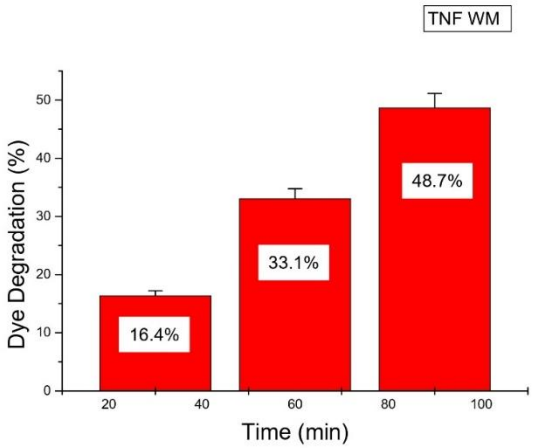

Fig. 16. Percentage degradation of RB 5 (10 ppm) with TiO_2 nanofibers. Error bars show standard deviations

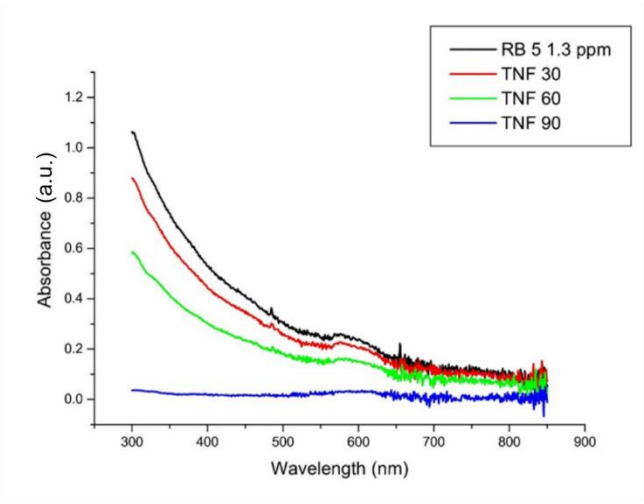

Fig. 17. Action of TiO_2 nanofibers incorporated PSF composite membrane on RB 5 dye degradation

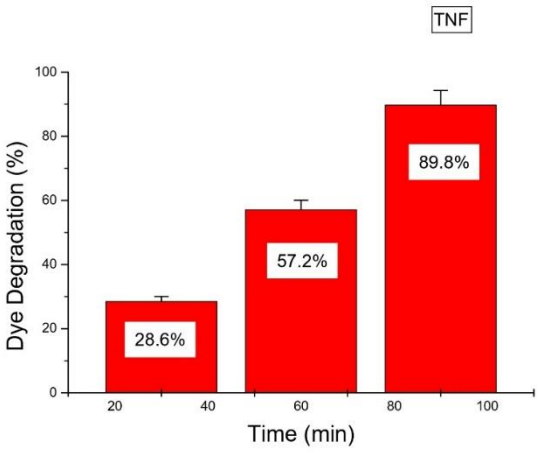

Fig. 18. Percentage degradation of RB 5 (1.3 ppm) with TiO_2 nanofibers – PSF membrane. Error bars show standard deviations

Figure 19 and 20 show the extent of 10 ppm RB 5 feed dye degradation at regular intervals of 30 mins conferred by TiO_2 nanotubes and nanofibers, respectively.

Figure 21 and 22 show the extent of 1.3 ppm RB 5 dye degradation at regular intervals of 30 mins conferred by TiO_2 nanotubes and nanofibers embedded with PSF membranes, respectively.

Our previous work [23] demonstrated the photocatalytic degradation of RB 5 using TiO_2 and $CaCO_3$ nanoparticles and their composite PSF membranes, where the results were noteworthy with respect to the nanoparticles compared to the membranes.

In this study, the nanomaterials-PSF blend membranes showed great efficiency in degrading the RB 5 dye, as demonstrated in the results above.

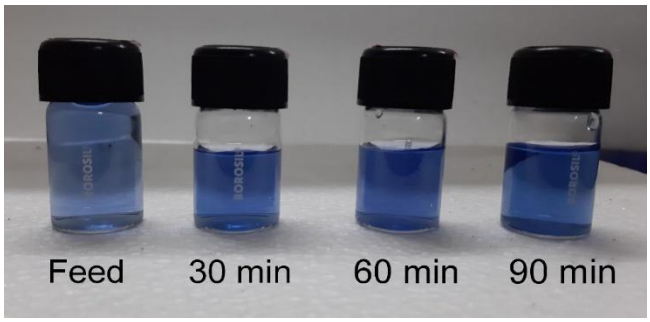

Fig. 19. Photograph of RB 5 Dye (10 ppm) feed and fractions collected at time intervals of 30 mins 10 in TiO_2 nanotubes photocatalysis

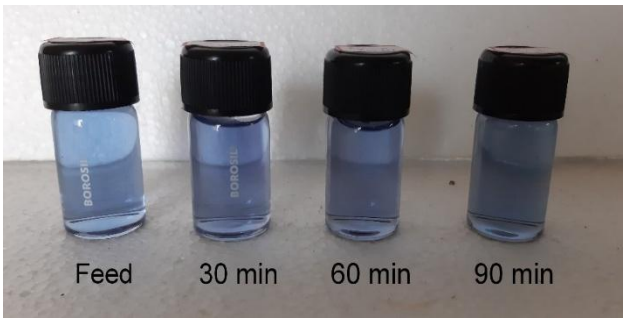

Fig. 20. Photograph of RB 5 Dye (10 ppm) feed and fractions collected at time intervals of 30 mins 10 in TiO_2 nanofibers photocatalysis

Fig. 21. Photograph of RB 5 Dye (1.3 ppm) degradation using TiO_2 nanotubes- PSF membrane

Fig. 22. Photograph of RB 5 Dye (1.3 ppm) degradation using TiO_2 nanofibers- PSF membrane

Table 1. A summary of the photocatalytic degradation of the RB 5 dye.

Materials	% of RB 5 dye degradation
TiO_2 nanotubes without membrane	18.6
TiO_2 nanotubes with membrane	80.2
TiO_2 nanofibers without membrane	48.7
TiO_2 nanofibers with membrane	89.8

4. Conclusion

The current work emphasizes the synthesis of TiO_2 nanotubes, nanofibers, and PSF membranes fabricated with synthesized nanotubes and nanofibers. The synthesis was confirmed by the interpretation of XRD and SEM results. UV-Visible spectroscopic studies showed that TiO_2 nanofibers embedded with PSF membranes were the most effective in decomposing RB 5 dye, followed by TiO_2 nanotubes embedded with PSF membranes. Without membranes, TiO_2 nanofibers were effective in action, whereas TiO_2 nanotubes were weak in breaking the RB 5 dye. The enhancement of strength in degrading is accounted for by the polymer matrix, along with the nanofibers and nanotubes. The industrial effluents containing remnants of RB 5 dye are toxic and harmful. Thus, this study is helpful in understanding the photocatalytic degradation of the RB 5 dye, which is responsible for various skin-related health problems, allergic reactions, bronchitis, and even an increased risk of cancer. Therefore, photocatalytic dye degradation of RB 5 is necessary and represents an important future perspective regarding health and the environment.

Acknowledgements

Authors are grateful to National Institute of Technology Karnataka (NITK), Surathkal for the lab, instrument facility, and UV-Visible Spectroscopic analysis. Sincere gratitude to Central Instrumentation Facility, Manipal Institute of Technology, Manipal, for the XRD and SEM analysis.

Author's contribution

Glanish Jude Martis: Formal analysis, Writing – original draft, software; **Arun M. Isloor:** Supervision, Conceptualization, Methodology, Writing – review & editing; **Sneha O:** Writing – original draft; **P. Satishkumar:** Methodology, Writing – review & editing; **Praveen S. Mugali:** Formal analysis.

Conflict of interest

No potential conflict of interest was reported by the authors.

Data availability

Not Applicable.

Funding

Self-funded.

References

[1] Al-Tohamy, R., Ali, S. S., Li, F., Okasha, K. M., Mahmoud, Y. A. G., Elsamahy, T., Jiao, H., Fu, Y. & Sun, J. (2022). A critical review on the treatment of dye-containing wastewater: Ecotoxicological and health concerns of textile dyes and possible remediation approaches for environmental safety. Ecotoxicology and environmental safety, 231, 113160. https://doi.org/10.1016/j.ecoenv.2021.113160

[2] Olisah, C., Adams, J. B., & Rubidge, G. (2021). The state of persistent organic pollutants in South African estuaries: A review of environmental exposure and sources. Ecotoxicology and Environmental Safety, 219, 112316. https://doi.org/10.1016/j.ecoenv.2021.112316

[3] Almroth, B. C., Cartine, J., Jönander, C., Karlsson, M., Langlois, J., Lindström, M., Lundin, J., Melander, N., Pesqueda, A., Rahmqvist, I., & Sturve, J. (2021). Assessing the effects of textile leachates in fish using multiple testing methods: From gene expression to behavior. Ecotoxicology and Environmental Safety, 207, 111523. https://doi.org/10.1016/j.ecoenv.2020.111523

[4] Teng, T. T., & Low, L. W. (2012). Removal of dyes and pigments from industrial effluents. In Advances in water treatment and pollution prevention (pp. 65-93). Dordrecht: Springer Netherlands. https://doi.org/10.1007/978-94-007-4204-8_4

[5] Satishkumar, P., Isloor, A. M., Rao, L. N., & Farnood, R. (2024). Fabrication of 2D vanadium MXene polyphenylsulfone ultrafiltration membrane for enhancing the water flux and for effective separation of humic acid and dyes from wastewater. ACS omega, 9(24), 25766-25778. https://doi.org/10.1021/acsomega.3c10078

[6] Hebbar, R. S., Isloor, A. M., Abdullah, M. S., Ismail, A. F., & Asiri, A. M. (2018). Fabrication of polyetherimide nanocomposite membrane with amine functionalised halloysite nanotubes for effective removal of cationic dye effluents. Journal of the Taiwan Institute of Chemical Engineers, 93, 42-53. https://doi.org/10.1016/j.jtice.2018.07.03

[7] Mohan, D., Sarswat, A., Ok, Y. S., & Pittman Jr, C. U. (2014). Organic and inorganic contaminants removal from water with biochar, a renewable, low cost and sustainable adsorbent–a critical review. Bioresource technology, 160, 191-202. https://doi.org/10.1016/j.biortech.2014.01.120

[8] Gupta, C., Pant, P., & Mishra, S. (2023). Removal of Organic and Inorganic Contaminants from Water Using Nanosponge Cyclodextrin Polyurethanes. In Nanosponges for Environmental Remediation (pp. 169-186). Cham: Springer Nature Switzerland. https://doi.org/10.1007/978-3-031-41077-2_8

[9] Akbar, S. A., & Khairunnisa, K. (2024). Seaweed-based biosorbent for the removal of organic and inorganic contaminants from water: a systematic review. In BIO Web of Conferences (Vol. 87, p. 02011). EDP Sciences. https://doi.org/10.1051/bioconf/20248702011

[10] Ghasemzadeh, K., Aghaeinejad-Meybodi, A., & Basile, A. (2017). Separation theory of silica membranes. In Current Trends and Future Developments on (Bio-) Membranes (pp. 65-95). Elsevier. https://doi.org/10.1016/B978-0-444-63866-3.00004-2

[11] Kajekar, A. J., Dodamani, B. M., Isloor, A. M., Karim, Z. A., Cheer, N. B., Ismail, A. F., & Shilton, S. J. (2015). Preparation and characterization of novel PSf/PVP/PANI-nanofiber nanocomposite hollow fiber ultrafiltration membranes and their possible applications for hazardous dye rejection. Desalination, 365, 117-125. https://doi.org/10.1016/j.desal.2015.02.028

[12] Hamid, N. A. A., Ismail, A. F., Matsuura, T., Zularisam, A. W., Lau, W. J., Yuliwati, E., & Abdullah, M. S. (2011). Morphological and separation performance study of polysulfone/titanium dioxide (PSF/TiO_2) ultrafiltration membranes for humic acid removal. Desalination, 273(1), 85-92. https://doi.org/10.1016/j.desal.2010.12.052

[13] Panda, S. R., & De, S. (2014). Preparation, characterization and performance of $ZnCl_2$ incorporated polysulfone (PSF)/polyethylene glycol (PEG) blend low pressure nanofiltration membranes. Desalination, 347, 52-65. https://doi.org/10.1016/j.desal.2014.05.030

[14] Kumar, R., Isloor, A. M., Ismail, A. F., & Matsuura, T. (2013). Performance improvement of polysulfone ultrafiltration membrane using N-succinyl chitosan as additive. Desalination, 318, 1-8. https://doi.org/10.1016/j.desal.2013.03.003

[15] Kumar, R., Isloor, A. M., Ismail, A. F., & Matsuura, T. (2013). Synthesis and characterization of novel water soluble derivative of chitosan as an additive for polysulfone ultrafiltration membrane. Journal of membrane science, 440, 140-147. https://doi.org/10.1016/j.memsci.2013.03.013

[16] Kumar, R., Isloor, A. M., Ismail, A. F., Rashid, S. A., & Al Ahmed, A. (2013). Permeation, antifouling and desalination performance of TiO_2 nanotube incorporated PSf/CS blend membranes. Desalination, 316, 76-84. https://doi.org/10.1016/j.desal.2013.01.032

[17] Padaki, M., Isloor, A. M., Kumar, R., Ismail, A. F., & Matsuura, T. (2013). Synthesis, characterization and desalination study of composite NF membranes of novel Poly [(4-aminophenyl) sulfonyl] butanediamide (PASB) and methyalated Poly [(4-aminophenyl) sulfonyl] butanediamide (mPASB) with Polysulfone (PSf). Journal of Membrane Science, 428, 489-497. https://doi.org/10.1016/j.memsci.2012.11.001

[18] Esmaili, Z., Sadeghian, Z., & Ashrafizadeh, S. N. (2024). Tailoring of $BiVO_4$ morphology for efficient antifouling of visible-light-driven photocatalytic ceramic membranes for oily wastewater treatment. Journal of Water Process Engineering, 67, 106145. https://doi.org/10.1016/j.jwpe.2024.106145

[19] Esmaili, Z., Sadeghian, Z., & Ashrafizadeh, S. N. (2023). Anti-fouling and self-cleaning ability of $BiVO_4$/rGO and $BiVO_4$/g-C_3N_4 visible light-driven photocatalysts modified ceramic

membrane in high performance ultrafiltration of oily wastewater. Journal of Membrane Science, 688, 122147. https://doi.org/10.1016/j.memsci.2023.122147

[20] Akrami, M. R., Sadeghian, Z., & Ashrafizadeh, S. N. (2025). Oily Wastewater Treatment via a Visible-light-responsive Slurry Membrane Photocatalytic Reactor Incorporating Bi_2WO_6-Based Photocatalysts. Chemical Engineering and Processing-Process Intensification, 110365. https://doi.org/10.1016/j.cep.2025.110365

[21] Golshenas, A., Sadeghian, Z., & Ashrafizadeh, S. N. (2020). Performance evaluation of a ceramic-based photocatalytic membrane reactor for treatment of oily wastewater. Journal of Water Process Engineering, 36, 101186. https://doi.org/10.1016/j.jwpe.2020.101186

[22] Sadeghian, Z., Zamani, F., & Ashrafizadeh, S. N. (2010). Removal of oily hydrocarbon contaminants from wastewater by γ-alumina nanofiltration membranes. Desalination and Water Treatment, 20(1-3), 80-85. https://doi.org/10.5004/dwt.2010.1154

[23] O, Sneha., Isloor, A. M., Martis, G. J., Bhat, S. P., & Mugali, P. (2024). Impact of TiO_2 and $CaCO_3$ nanoparticles and their incorporation in polysulfone composite membrane on photocatalytic degradation of RB 5. Advances in Environmental Technology, 10(4), 315-325. https://doi.org/10.22104/aet.2024.6957.1907

[24] Yousefi, V., & Kariminia, H. R. (2024). The optimization of reactive black 5 dye removal using Coprinus cinereus peroxidase (CIP). Advances in Environmental Technology, 10(2), 85-101. https://doi.org/10.22104/aet.2024.6444.1787

[25] Qu, X., Alvarez, P. J., & Li, Q. (2013). Applications of nanotechnology in water and wastewater treatment. Water research, 47(12), 3931-3946. https://doi.org/10.1016/j.watres.2012.09.058

[26] Shenvi, S. S., Isloor, A. M., Ismail, A. F., Shilton, S. J., & Al Ahmed, A. (2015). Humic acid based biopolymeric membrane for effective removal of methylene blue and rhodamine B. Industrial & Engineering Chemistry Research, 54(18), 4965-4975. https://doi.org/10.1021/acs.iecr.5b00761

[27] Razmjou, A., Resosudarmo, A., Holmes, R. L., Li, H., Mansouri, J., & Chen, V. (2012). The effect of modified TiO_2 nanoparticles on the polyethersulfone ultrafiltration hollow fiber membranes. Desalination, 287, 271-280. https://doi.org/10.1016/j.desal.2011.11.025

[28] Moslehyani, A., Ismail, A. F., Othman, M. H. D., & Isloor, A. M. (2015). Novel hybrid photocatalytic reactor-UF nanocomposite membrane system for bilge water degradation and separation. RSC Advances, 5(56), 45331-45340. https://doi.org/10.1039/C5RA01491C

[29] Andreozzi, R., Caprio, V., Insola, A., & Marotta, R. (1999). Advanced oxidation processes (AOP) for water purification and recovery. Catalysis today, 53(1), 51-59. https://doi.org/10.1016/S0920-5861(99)00102-9

[30] Fujishima, A., Rao, T. N., & Tryk, D. A. (2000). Titanium dioxide photocatalysis. Journal of photochemistry and photobiology C: Photochemistry reviews, 1(1), 1-21. https://doi.org/10.1016/S1389-5567(00)00002-2

[31] Thakur, V. K., & Voicu, S. I. (2016). Recent advances in cellulose and chitosan based membranes for water purification: A concise review. Carbohydrate polymers, 146, 148-165. https://doi.org/10.1016/j.carbpol.2016.03.030

[32] Majid, D., Al Kholif, M., Arif, M. N., Sutrisno, J., & Zhang, J. W. (2025). Eco-friendly solutions for urban wastewater: evaluating constructed wetlands and filtration methods. Advances in Environmental Technology, 11(2), 182-194. https://doi.org/10.22104/aet.2025.6887.1887

[33] Yanqoritha, N., Piska, F., Ginting, B. N. B., & Mitha, N. (2024). Using biofilter aerobic reactor for optimizing the hydraulic loading rate in nitrification process for tofu-manufacturing wastewater management. Advances in Environmental Technology, 10(4), 326-338. https://doi.org/10.22104/aet.2024.6855.1882

[34] Serbanescu, O. S., Voicu, S. I., & Thakur, V. K. (2020). Polysulfone functionalized membranes: Properties and challenges. Materials today chemistry, 17, 100302. https://doi.org/10.1016/j.mtchem.2020.100302

[35] Liu, W., Gao, J., Zhang, F., & Zhang, G. (2007). Preparation of TiO_2 nanotubes and their photocatalytic properties in degradation methylcyclohexane. Materials Transactions, 48(9), 2464-2466. https://doi.org/10.2320/matertrans.MRA2007616

[36] Zhang, F. B., & Li, H. L. (2007). Hydrothermal synthesis of TiO_2 nanofibers. Materials Science and Engineering: C, 27(1), 80-82. https://doi.org/10.1016/j.msec.2006.02.001

[37] Poulios, I., & Tsachpinis, I. (1999). Photodegradation of the textile dye Reactive Black 5 in the presence of semiconducting oxides. Journal of Chemical Technology & Biotechnology: International Research in Process, Environmental & Clean Technology, 74(4), 349-357. https://doi.org/10.1002/(SICI)1097-4660(199904)74:4<349::AID-JCTB5>3.0.CO;2-7

[38] Kumar, R., Isloor, A. M., Ismail, A. F., Rashid, S. A., & Al Ahmed, A. (2013). Permeation, antifouling and desalination performance of TiO_2 nanotube incorporated PSf/CS blend membranes. Desalination, 316, 76-84. https://doi.org/10.1016/j.desal.2013.01.032

How to cite this paper:

Martis, G. J., Isloor, A. M., O, S., Satishkumar, P. & Mugali, P. S. (2026). Harnessing the impact of TiO_2 nanotubes, TiO_2 nanofibers and their incorporation in Polysulfone composite membrane for the photocatalytic degradation of Reactive Black 5. Advances in Environmental Technology, 12(1), 63-75. DOI: 10.22104/aet.2025.7536.2113